7 Outdoor thermal comfort within different building blocks

Part B studied indoor thermal comfort and energy efficiency of different building blocks. It then, focused on different courtyard buildings and showed the optimum ways of courtyard design from an indoor perspective.

Chapter 7 begins a new part of the dissertation on outdoor thermal comfort. This chapter is parallel to Chapter 4 in which different building block forms were studied. In this chapter, outdoor thermal comfort resulting from different urban forms will be investigated. The aim is to explore whether a courtyard is capable to provide a more comfortable microclimate in comparison with the other forms. The study is based on the simulation of the hottest day in a reference year in the Netherlands. The simulation software is validated through a field measurement inside an actual courtyard on the campus of Delft University of Technology.

Outdoor thermal comfort within five different urban forms in the Netherlands[1]

Mohammad Taleghani *[1], *Laura Kleerekoper* [1], *Martin Tenpierik* [1], *Andy van den Dobbelsteen* [1]

1 Faculty of Architecture and the Built Environment, Delft University of Technology, Delft, the Netherlands

Abstract

Outdoor thermal comfort in urban spaces is known as an important contributor to pedestrians' health. The urban microclimate is also important more generally through its influence on urban air quality and the energy use of buildings. These issues are likely to become more acute as increased urbanisation and climate change exacerbate the urban heat island effect. Careful urban planning, however, may be able to provide for cooler urban environments. Different urban forms provide different microclimates with different comfort situations for pedestrians. In this paper, singular East-West and North-South, linear East-West and North-South, and a courtyard form were analysed for the hottest day so far in the temperate climate of the Netherlands (19th June 2000 with the maximum 33°C air temperature). ENVI-met was used for simulating outdoor air temperature, mean radiant temperature, wind speed and relative humidity whereas RayMan was used for converting these data into Physiological Equivalent Temperature (PET). The models with different compactness provided different thermal environments. The results demonstrate that duration of direct sun and mean radiant temperature, which are influenced by urban form, play the most important role in thermal comfort. This paper also shows that the courtyard provides the most comfortable microclimate in the Netherlands in June compared to the other studied urban forms. The results are validated through a field measurement and calibration.

Keywords

Outdoor thermal comfort, urban forms, PET, ENVI-met, Netherlands.

1 Published as: Taleghani M., Kleerekoper, L, Tenpierik M., Dobbelsteen A., "Outdoor thermal comfort within five different urban forms in the Netherlands", Building and Environment, Accepted for publication with DOI: http://dx.doi.org/10.1016/j.buildenv.2014.03.014.

§ 7.1 Introduction

Thermal comfort is defined as 'that condition of mind which expresses satisfaction with the thermal environment' [1]. Since the 1980s, studies of thermal comfort in the outdoor environment have grown in number because of increased attention for pedestrians in urban canyons, plazas and squares. This led to a great number of researches addressing microclimate design parameters based on pedestrians' thermal comfort [2-9]. Thermal comfort in the outdoor environment is mainly related to thermo-physiology, i.e. physiology and the heat balance of the human body [10]. This field of study connects urban and landscape designers to bio-meteorology (more focus on pedestrians) and climatology (more focus on climate). Both bio-meteorologists and climatologists had important roles in developing thermal comfort indices such as the physiological equivalent temperature (PET) [11] and the universal thermal climate index [12]. With regard to different urban forms these indices have been well studied for hot arid and humid climates, but to a lesser extent for cooler environments, probably because in these climates people spend most of their times indoors. But considering climate change and the rise of global temperature makes outdoor thermal comfort more urgent [13, 14].

The Netherlands has a temperate climate. Winters are milder than other climates in similar latitudes (and usually very cloudy) and summers are cool due to cool ocean currents. This country is faced with the effects of rapid climate change such as global temperature rise. Among different efforts, an appropriate urban design can help to mitigate heat stress for pedestrians. In this chapter, five basic microclimates formed by simple urban forms are subject to analyses from a normal pedestrian's thermal comfort perspective. These analyses were conducted in the context of a representative meteorological city in the Netherlands: De Bilt. The aim of the study is to show which of the urban forms can provide a more comfortable microclimate on the hottest day of a year. Understanding the thermal behaviour of these microclimates allows landscape and urban designers to have clear guidelines for planning and design at their proposal.

§ 7.1.1 Outdoor thermal comfort indices

Howard [15] was the first who suggested to consider the effect of urban form on microclimate. In 1914 Hill, Griffith [16] made a big thermometer that indicated the influence of mean radiant temperature, air temperature and air velocity. Furthermore, Dufton [17] defined the equivalent temperature (T_{eq}) in 1929. This equivalent temperature, however, was only in use for a short period because environmental variables were not accounted for in the algorithms [18, 19]. In addition, ASHRAE

proposed and used the effective temperature (ET) from 1919 till 1967 [20]. In 1971, Gagge introduced ET* which was more accurate than ET because it simultaneously covered radiation, convection and evaporation. Around the same time, Fanger [21] developed theories of human body heat exchange based on PMV (Predicted Mean Votes) or PPD (Predicted Percentage Dissatisfied). Later on, this theory became the basis for indoor thermal comfort standards such as ISO 7730-1984 and ASHRAE 55-1992. Tahbaz [22] and Cohen, Potchter [7] have divided thermal indices into cold and hot climates:

a Hot climates: Heat Stress Index (HIS) [23], Wet Bulb Globe Temperature (WBGT) [24], Discomfort Index (DI) [25], Index of Thermal Stress (ITS) [26], New Effective Temperature (ET*) [27], Skin Wettedness [28], Heat Index (HI) [29] and Tropical Summer Index (TSI) [30].

b Cold climates: Wind Chill Index (WCI) and Wind Chill Equivalent Temperature (WCET) [31].

As a next step, the need for indices applicable to all climates and seasons led to a number of universal indices such as the Standard Effective Temperature (SET) [32], Perceived Temperature (PT) [33], Outdoor Standard Effective Temperature (OUT_SET) [34], Physiological Equivalent Temperature (PET) [35, 36] and Universal Thermal Climate Index (UTCI) [37-39].

PET, or the physiological equivalent temperature (expressed by °C), tries to simplify the outdoor climate as an index for a lay person. This index is based on the Munich energy balance model for individuals (MEMI) [35, 36, 40] which is a thermo-physiological heat balance model. Such a model takes into account all basic thermoregulatory processes, such as the constriction or dilation of peripheral blood vessels and the physiological sweat rate. In detail, such models are based on the following equation:

$$S = M \pm W \pm R \pm C \pm K - E - RES \quad (1)$$

Where S is heat storage, M is metabolism, W is external work, R is heat exchange by radiation, C is heat exchange by convection, K is heat exchange by conduction, E is heat loss by evaporation, and RES is heat exchange by respiration (from latent heat and sensible heat).

Actually, PET provides the equivalent temperature of an isothermal reference environment with a 12 hPa water vapour pressure (50% at 20°C) and air velocity of 0.1 m/s, at which the heat balance of a lay person is maintained with core and skin temperature equal to those under the conditions in question. PET uses PMV as assessment scale, making it similar to a comfort index [11, 41]. Finally, Matzarakis and Amelung [42] showed that PET is an accurate index for the assessment of the effects of climate change on human health and well-being. Last but not least, PET has the most important variables for human thermal comfort such as airflow, air temperature,

radiant temperature and humidity. Moreover, the outcomes give a clear indication on the comfort temperature because it is still in degrees and therefore logical also for people that are no experts in meteorology. In this chapter, PET – which has been tested and verified for the climate of North and West Europe [11, 36, 42] – is elaborated and used for the calculations of thermal comfort.

PMV	PET °C	Thermal Perception	Grade of physiological stress
-3.5	4	Very cold	Extreme cold stress
-2.5	8	Cold	Strong cold stress
-1.5	13	Cool	Moderate cold stress
-0.5	18	Slightily cool	Slight cold stress
0.5	23	Comfortable	No thermal stress
1.5	29	Slightly warm	Slight heat stress
2.5	35	Warm	Moderate heat stress
3.5	41	Hot	Strong heat stress
		Very hot	Extreme heat stress

Table 1
Ranges of the thermal indexes predicted mean vote (PMV) and physiological equivalent temperature (PET) for different grades of thermal perception by human beings and physiological stress on human beings; internal heat production: 80 W, heat transfer resistance of the clothing: 0.9 clo [11].

§ 7.1.2 Urban typology study

Studies of the effect of urban form on outdoor microclimate are more recent than studies of indoor climate. Olgyay [43] and Oke [2] were the first scholars who discussed relationships between architects and urban designers from a climatologic point of view, focussing on the interactions between building and microclimate design. Givoni [3] deliberates the impacts of urban typologies in different climates. Steemers et al. [44] proposed six archetypal generic urban forms for London and compared the incident of solar radiation, built potential and daylight admission. Their study was followed by Ratti et al. [45] for the city of Marrakech. They concluded that large courtyards are environmentally adequate in cold climates, where under certain geometrical conditions they can act as sun concentrators and retain their sheltering effect against cold winds. Bourbia and Awbi [46] [47] examined the effect of the height-to-width ratio (H/W) and the sky view factor (SVF) of a building cluster on the outdoor air and surface temperature in the city of El-Oued in Algeria. SVF is the extent of sky observed from a point as a proportion of the total possible sky hemisphere. They concluded that by controlling the sky view factor and street architecture it is possible to prevent high temperatures in urban canyons and that these therefore have an effect on a local scale

rather than city scale. A comprehensive study on urban courtyards at a latitude of 26-34°N was done by Yezioro et al. [48] using the SHADING program. They showed that, for cooling purposes, the best direction of a rectangular courtyard was North-South (NS, i.e. with the longer facades on East and West), followed by NW-SE, NE-SW, EW (in this order). They found that the NS direction had the shortest duration of direct sun light in the centre of the courtyard. This finding is in accordance with climates (or seasons) in which less sun is desirable. They also investigated summer thermal comfort, and showed that, although the air temperature difference between shaded and unshaded areas was only 0.5 K, the mean radiant temperature was different up to 30 K [49].

Okeil [50] developed a built form named the Residential Solar Block (RSB), which was later compared with a slab and a pavilion court [51]. The RSB was found to lead to an energy-efficient neighbourhood layout for a hot and humid climate. Ali-Toudert and Mayer [52, 53] used the microclimate model ENVI-met to simulate the outdoor thermal comfort in the hot dry climate of Ghardaia, Algeria. They also studied the effect of different orientations of the urban canyon. It was concluded that the air temperature slightly decreases (and that the PET improves) when the aspect ratio of building height/canyon width (H/W) increases. Johansson [54] conducted measurements in Fez, Morocco, and found that a compact urban design with deep canyons is suitable for summer; however, in winter a wider canyon is more favourable for passive solar heating. Bourbia and Boucheriba [55] did several site measurements in Constantine, Algeria. They measured outdoor air and surface temperatures on seven sites with varying height-to-width ratios between 1 and 4.8 and sky view factors between 0.076 and 0.580. They observed that the higher the height-to-width ratio, the lower the surface and air temperatures. Consequently, in the hot arid climate, the higher the sky view factor, the higher the outdoor air temperature. The role of vegetation and appropriate microclimate design in hot and arid climates are also extensively discussed by Erell et al. [56, 57] and Taleghani et al. [58, 59].

In the temperate climate of Western Europe, Herrmann and Matzarakis [5] simulated urban courtyards with different orientations in Freiburg, Germany. They showed that mean radiant temperature (T_{mrt}) has the highest value for North–South and lowest for East–West orientation at midday and during the night. During the night, mean radiant temperatures were very similar, but the orientation of the courtyard can affect the time of the first increase in T_{mrt} (due to direct sun) in the morning. Müller and Kuttler [60] in a quantification of the thermal effects of several adaptation measures and varying meteorological parameters using ENVI-met in an inner-city neighbourhood (Oberhausen, Germany) showed that increasing wind speed in summer can reduce PET up to 15°C. Thorsson and Lindberg [61] in a simulation study for a high latitude city in Sweden (Gothenburg) found out that open areas are warmer than adjacent narrow street canyons in summer, but cooler in winter. They also showed that a densely built structure mitigates extreme swings in T_{mrt} and PET, improving outdoor comfort

conditions both in summer and in winter. In the Netherlands (52°N on average), few studies have addressed PET or other outdoor thermal comfort indices. Among these, Taleghani et al. [62, 63] showed the effect of different urban models on indoor energy demand. They found out that dwellings in a courtyard layout are more protected and need 22% less heating energy in winter rather than a detached free standing building. They also showed different orientations and materials have a significant effect on outdoor thermal comfort of courtyards [64]. Furthermore, van Esch et al. [65] compared urban canyons with street widths of 10, 15, 20 and 25 meters, and E-W and N-S directions. They concluded that the E-W canyons do not receive sun on the 21st of December, whilst during summer time and in the morning and afternoon, they have direct sun. At noon the sun is blocked. On the shortest day, the N-S canyons get some sun for a short period (even the narrowest canyon) and are fully exposed to the sun in the mornings and afternoons.

§ 7.2 Methodology

For this chapter, five urban forms were selected to be assessed in terms of thermal comfort in the temperate climate of the Netherlands. The urban forms are simplified and taken from the study of Ratti and Raydan [45] and existing examples in the Dutch urban contexts (Figure 1). As Figure 2 shows, the study aims to investigate thermal comfort for a pedestrian in the centre of the urban forms. In this regard, the hottest day of the Dutch reference year [66] is considered for simulations with ENVI-met. This program simulated the microclimates' data (e.g. mean radiant temperature, air temperature, relative humidity, etc.) and the output was 'measured' in points at 1.40 meter height in the centre of the urban forms. As the next step, these data were entered into RayMan [67] to calculate the physiological equivalent temperature (PET) based on the sky view factors of the central points. The outdoor thermal comfort of the points will be discussed and compared in this chapter.

Figure 1
Singular (left) linear (middle) and courtyard (right) urban forms in the Netherlands.

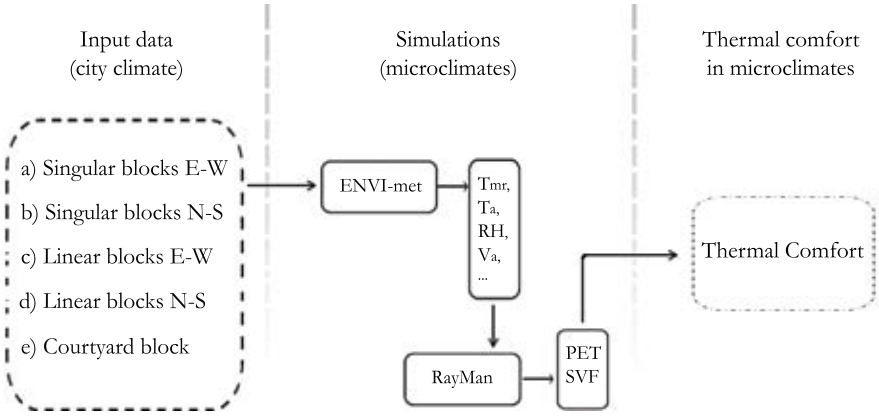

Figure 2
The research method. The simulations are done for the hottest day so far in the Netherlands, 19th of June 2000.

§ 7.2.1 Models

The five forms of urban open spaces considered in the study discussed were derived from Martin and March [68], Steemers and Baker [44] and Ratti and Raydan [45] (Figure 3). The open spaces surround 8 blocks, these blocks are 10 x 10 m^2 each with a height of 9 m (3 storeys). The receptor (the point considered for thermal comfort) is located in the centre of the canyon or courtyard at a height of 1.40 m. The five urban forms are:

a) Singular blocks E-W; and b) Singular blocks N-S; c) Linear blocks E-W; and d) Linear blocks N-S: these models are the same as form a and b but now the building blocks are connected to each other, forming a set of terraced houses; e) A courtyard block: this block again consists of the same 8 modules forming an internal courtyard of 10 m^2.

The material of walls are assumed brick (U value of 0.31 W/m^{2}k). The pavements are concrete, and the roofs have the albedo of asphalt.

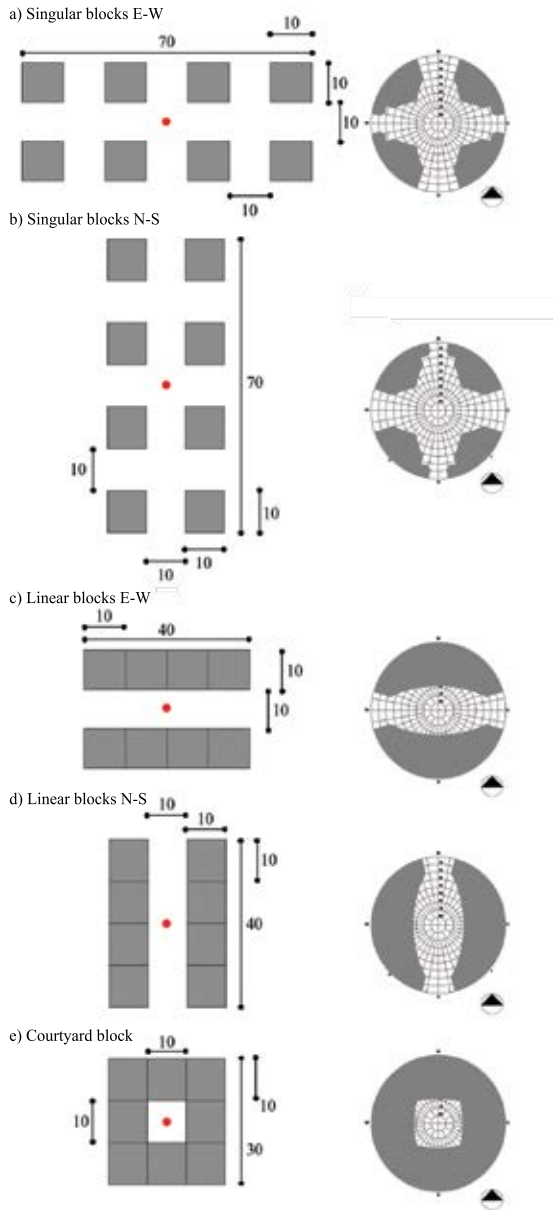

Figure 3
Left: the five models and the positions of the reference points (the numbers are in meter); Right: the Sky View Factor (SVF) of all the forms, a) and b) 0.605, c) and d) 0.404 and e) 0.194) (calculated and produced by RayMan).

§ 7.2.2 Simulations

For the study presented, 19th of June 2000 as the most extreme hot day was selected to check the potential of the urban forms in providing acceptable outdoor thermal comfort in summer. In this regard, the simulations were done by means of the following software:

A ENVI-met 3.1:

This program is a three-dimensional microclimate model designed to simulate the interaction between surfaces, plants and air in an urban environment with a typical resolution of 0.5 to 10 meters in space and 10 second in time. In this chapter, the time step of 1 hour is used. With this programme, the air temperature (°C), vapour pressure (hPa), relative humidity (%), wind velocity (m/s) and mean radiant temperature (°C) of the receptors in the centre of models can be calculated [69]. A limitation regarding this program is the lack of PET in the outputs. As Figure 3 illustrates, thermal comfort information will be gathered in receptor points. Regarding the wind boundry conditions, ENVI-met makes the height of the boundry 3 times more than the height of the tallest building. Therefore, in the simulation of the five urban forms, the height of the boundry is 36 meter.

The ENVI-met model is chosen because it is the most complete model in terms of the calculation of human comfort. The generated output contains the four main thermal comfort parameters: air temperature, mean radiant temperature (T_{mrt}), wind speed and relative humidity. Another model that calculates outdoor conditions is the SOLWEIG model developed by Göteborg University [70]. The SOLWEIG model is a radiation model that is very accurate in predicting the T_{mrt}, but does not provide output of the three other thermal comfort parameters. There are also computational fluid dynamics (CFD) models like, ANSYS Fluent, which are developed to predict air flow and turbulence which are extended with a radiation and heat balance and an evaporation module [71]. Modelling with Fluent is very precise and used to test the aerodynamics of, for example, vehicles or to calculate flow in indoor spaces. Modelling and calculation time take much longer than with ENVI-met, while the obtained accuracy is not relevant at street level. The RayMan model, in contrast with CFD modelling, has a very short running time. The model is a radiation model and generates the T_{mrt} like the SOLWEIG model, however does not include multiple reflection between buildings. A large advantage of the model is the possibility to generate output in common thermal comfort indexes like the PET and PMV [67].

Other models that are used to simulate thermal comfort conditions are Ecotect, Design Builder and Transit. Ecotect is specialised in analysing daylight conditions, Design

Builder allows to check energy, carbon, lighting and comfort performance and Transit has a strong energy focus. These models are all developed to calculate indoor spaces and therefore not suitable for the analyses of thermal comfort at street level.

Figure 4 shows a schematic overview of the ENVI-met model layout. The 3D model in ENVI-met is encapsulated within a 1D model that creates the boundary conditions. This 1D model simulates the atmospheric processes up to 2500m height. The 3D model has grid cells, and the size of cells are based on the resolution in Input File. In the vertical direction, the first (lowest) five cells have a vertical extension of $\Delta z=0.2\ \Delta z$ to increase the accuracy of surface processes calculations [72].

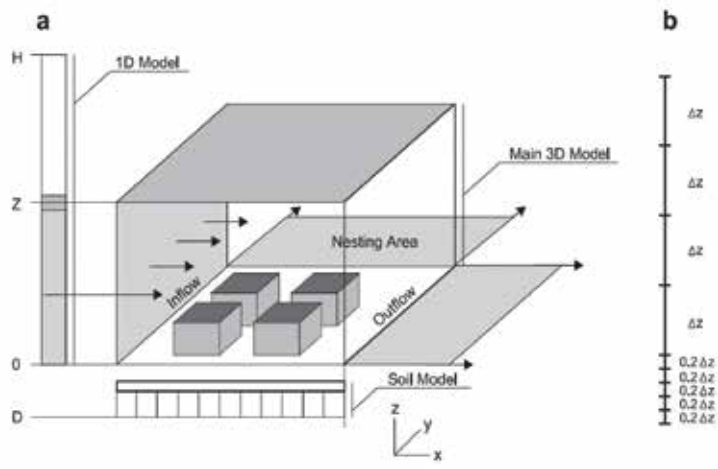

Figure 4
(a)- A schematic overview of the ENVI-met model layout. Z shows the height of the main 3D model, H the height of the 1D model, and D the depth of the model (soil). (b) [72].

The model is composed of four main systems: soil, vegetation, atmosphere and building. The basic equations from the physical model are related to a) mean air flow, b) temperature and humidity, c) turbulance and exchange processes, and d) radiative fluxes. The complete model system includes a number of additional moduls such as biometeorological or particle dispersion models. Here, mean air flow is described as an example:

The basic concept to describe three-dimensional turbulent flow is given by the non-hydrostatic incompressible NavierStokes equations in the Boussinesq- approximated form (2.1 – 2.3):

$$\frac{\partial u}{\partial t} + u_i \frac{\partial u}{\partial x_i} = -\frac{\partial p^{'}}{\partial x} + K_m \left(\frac{\partial^2 u}{\partial x_i^2} \right) + f(v - v_g) - S_u \tag{2.1}$$

$$\frac{\partial v}{\partial t} + u_i \frac{\partial v}{\partial x_i} = -\frac{\partial p^{'}}{\partial y} + K_m \left(\frac{\partial^2 v}{\partial x_i^2} \right) - f(u - u_g) - S_v \tag{2.2}$$

$$\frac{\partial w}{\partial t} + u_i \frac{\partial w}{\partial x_i} = -\frac{\partial p^{'}}{\partial z} + K_m \left(\frac{\partial^2 w}{\partial x_i^2} \right) + g \frac{\theta(z)}{\theta_{ref}(z)} - S_w \tag{2.3}$$

with u_i= (u, v, w), u_i = (x, y, z) for i= 1, 2, 3.

As the flow is incompressible in ENVI-met, $^{l}\rho$ does not change for any fluid parcel, and $D\rho/Dt = 0.$. Therefore, the Continuity equation is reduced to:

$$\frac{\partial u}{\partial x} + \frac{\partial v}{\partial y} + \frac{\partial w}{\partial z} = 0 \tag{3}$$

where,

$f\,(=10^4\ \mathrm{sec}^{-1})$ is the Coriolis parameter,
p' is the local pressure perturbation, and
θ is the potential temperature at level z.

The reference temperature θ_{ref} should represent average mesoscale conditions and is provided by a one-dimensional model running parallel to the main model. Although in this chapter vegetation is not simulated in the models, the local source/sink terms S_u, S_v and S_w describe the loss of wind speed due to drag forces at vegetation elements [73]. Here, mean air flow is described, and the calculations of temperaure, humidity, turbulance and exchange processes are extensively explained by Bruse and Fleer [74].

B RayMan 1.2

This programme considers outdoor conditions and calculates human thermal comfort. In this research human comfort was analysed through the calculation of PET. Sky views are also generated to provide a better understanding of the relation between the amount of insolation and thermal comfort. As input for these calculations, personal data (height, weight, age, sex), clothing (clo) and activity (W) are needed. Tables 2 and 3 give the climate conditions and other input data for the simulations.

Simulation day	19.06.2000
Simulation period	21 hours (04:00-01:00)
Spatial resolution	1m horizontally, 2m vertically
Wind speed	3.5 m/s
Wind direction (N=0, E=90)	187 °
Relative humidity (in 2m)	59 %
Indoor temperature	293 °K (=20 °C)
Heat transmission	0.31 W/m²K (walls), 0.33 W/m²K (roofs)
Albedo	0.1 (walls), 0.05 (roofs)

Table 2
Conditions used in the simulations with ENVI-met 3.1.

Simulation day	19.06.2000
Cloud coverage	0 Octa
Activity	80 W
Clothing	0.5 clo
Personal data	1.75 m, 75 kg, 35 years, male

Table 3
Conditions used in the simulations with RayMan 1.2.

Finally, the two software programmes discussed above were employed for the calculations of thermal comfort. Firstly, ENVI-met was used to generate T_{mrt}, air temperature, wind speed, and relative humidity of the receptor points. Secondly, the parameters mentioned were used in RayMan, in order to calculate the PETs for a normal pedestrian.

§ 7.2.3 Weather data

The climate of De Bilt (52°N, 4°E), which is representative for the Netherlands, is known as a temperate climate based on the classification of Köppen-Geiger [75]. The prevailing wind direction is South-West. The mean annual dry bulb temperature is 10.5 °C. Figure 5 presents the frequency distribution of different comfort classifications derived from the physiological equivalent temperature (PET) for the reference Dutch year NEN5060 [66]. According to this standard, every month of the reference year is represented by a specific year which is considered representative of the period from 1986 until 2005. The calculations of PET are done via RayMan for a normal 35-year

old male person of 1.75 m high and 75 kg, with a metabolic rate of 80 Watt. An activity level of 80 W arises when a normal person is walking with 1.2 m/s.

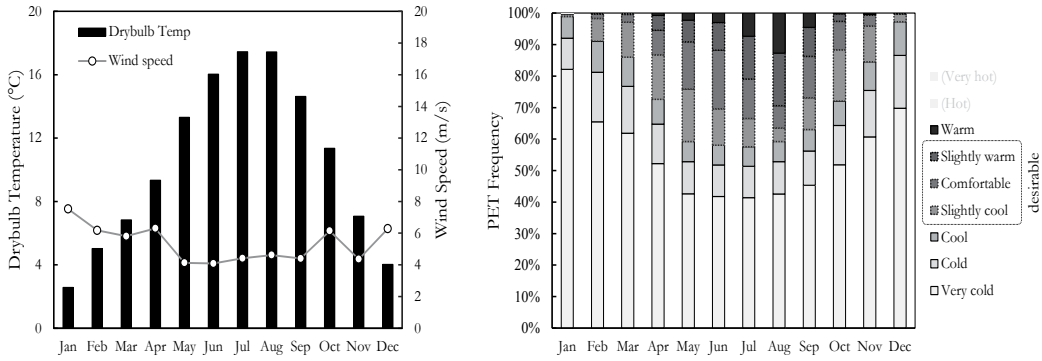

Figure 5
Left, drybulb outdoor temperature and wind speed of De Bilt. Right, Percentage frequency of PET in the climate of De Bilt (in the open field and outside an urban form). The comfort ranges, from slightly cool to slightly warm, are highlighted. The comfort range is between 18°C and 23°C, and has occurred in 10 per cents of the year.

§ 7.2.4 Validation of ENVI-met

§ 7.2.4.1 Measurement versus simulation

In this step, one ENVI-met model (the courtyard shape as a sample) was validated through a comparison between field measurements and simulation results. The measurements were done within a courtyard building on the campus of Delft University of Technology, Delft, the Netherlands (Figure 6-a,b). A wireless Vantage Pro2 weather station was used to measure drybulb air temperature with an interval of 5 minutes (Figure 6-c). The sensor of air temperature was protected by a white shield to minimise the effect of radiation. The courtyard environment was measured for 16 days in September 2013. Two random days, September 22nd and 25th were selected for ENVI-met simulation. The weather data for the simulations were taken from a weather station located 300 meters from the courtyard. The data from simulations and measurements are compared in Figure 7 to show the accuracy of the simulation results. To do these simulations, an ENVI-met Area Input File and a Configuration

File are needed.The simulation input data are presented in Table 4 (like the Area Input File). For the Configuration file, an area of 289*417 m is modeled. The effect of the neghibouring environment on the courtyard affects the output data. So, the surrounding vegetations, pavements, canals and buildings are also included in the model. To have more accurate results, the simulations are done 3 hours before the day in question (at 21:00 PM of the last day).

	First day	Second day
Simulation day	22.09.2013	25.09.2013
Simulation period	28 hours	28 hours
Spatial resolution	3m horizontally, 2m vertically	3m horizontally, 2m vertically
Initial air temperature	15.6°C	14°C
Wind speed	1.0 m/s	1.1 m/s
Wind direction (N=0, E=90)	245°	180°
Relative humidity (in 2m)	94 %	87 %
Indoor temperature	20°C	20°C
Thermal conductance	0.31 W/m²K (walls), 0.33 W/m²K (roofs)	0.31 W/m²K (walls), 0.33 W/m²K (roofs)
Albedo	0.10 (walls), 0.05 (roofs)	0.10 (walls), 0.05 (roofs)

Table 4
The conditions used in the validation simulations.

The measured and simulated dry bulb temperatures during 22nd and 25th of September are compared in Figure 7 (respectively a and b). On the first day, the patterns of air temperature between the measurement and the simulation are more or less the same, and, the peak of T_a according to the simulation is 0.5°C higher than according to the measurement. On the second day, the peaks of the hottest hour are different in number and in time, and, the peak of T_a according to the measurement is 1.2°C higher than according to the simulation. The root mean square deviation (RMSD) is a frequently used measure of the differences between values predicted by a model or an estimator (here the simulations) and the values actually observed (here the measurements). The RMSD of the dry bulb temperature between simulation and measurement on the first day is 0.7°C, and on the second day is 1.3°C. One of the reasons for the disagreement between the results could be the fact that ENVI-met does not include sky situation and cloudiness in its input parameters. Moreover, Ali-Toudert and Mayer [53] state that ENVI-met underestimates the temperatures at nights because of the missing heat storage in building surfaces. This is visible in Figure 7-a between 21:00 PM and 7:00 AM, and in Figure 7-b between 15:00 PM and 24:00. Figure 7-c shows the scatterplot of measured versus simulated Ta. The correlation coefficient between the two sets of data is 0.80.

a b c

Figure 6
a) The location of Delft as the place of validation, and De Bilt as the representative climate for the Netherlands (used in further simulations), b) the weather station (Vantage Pro2) used for measurement in situ, c) a view from inside the courtyard.

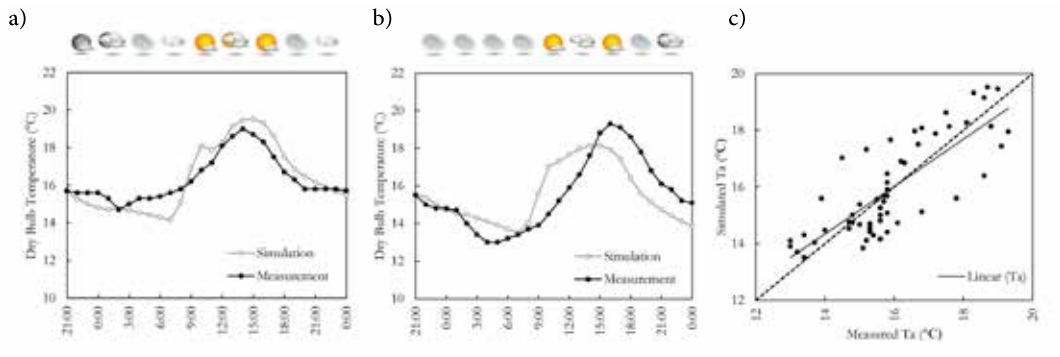

Figure 7
Comparison of simulation (ENVI-met) results with measurements on September 22nd (a) and September 25th (b). The mentioned data are compared in a scatterplot (c).

§ 7.2.4.2 Computational domain size sensitivity check

To check the accuracy of the ENVI-met models, the courtyard shape (as a sample of models in Figure 3) is modelled with two different domain sizes (180*180 m^2 and 90*90 m^2). As it is shown in Figure 8-a, a courtyard model with 8 similar blocks in its surrounding is modelled in the 180*180 m^2 domain size. Then, the same model and surface characteristics is simulated also in the 90*90 m^2 domain size withought

neighbouring blocks (Figure 8-b). The height of the boundries are both 52 m (which is four times of the tallest building in the models). If the results of the couryard model in the context of these two different domain sizes are identical, further simulations could be done with 90*90 m^2 (the smaller grid size) to reduce the simulation time.

For this comparison, the air temperature within the courtyards are compared. The simulations are done under the conditions mentioned in Table 2 (with the same weather data in Area Input Files). Figures 8-c and 8-d show the air temperature of the courtyards (height of 1.6 m) at 16:00 of the simulation day in 180*180 m^2 and 90*90 m^2 domain size, respectively. Figure 8-e shows the comparison of the air temperature for the two domain sizes, and Figure 8-f shows both results as function of each other. Since the air temperatures in the two models do not exactly match, the trendline in Figure 8-f is not perfectly 45°. This shows that there is a deviation between the two situations (domain sizes). In fact, the root mean square deviation of the two situations is 0.32°C. The average root mean square deviations for air temperature in the courtyard models are 0.26°C. This shows that further simulations with a 90*90 m^2 domain only, thus withought similar urban blocks, introduces a small but acceptable deviation in air temperature.

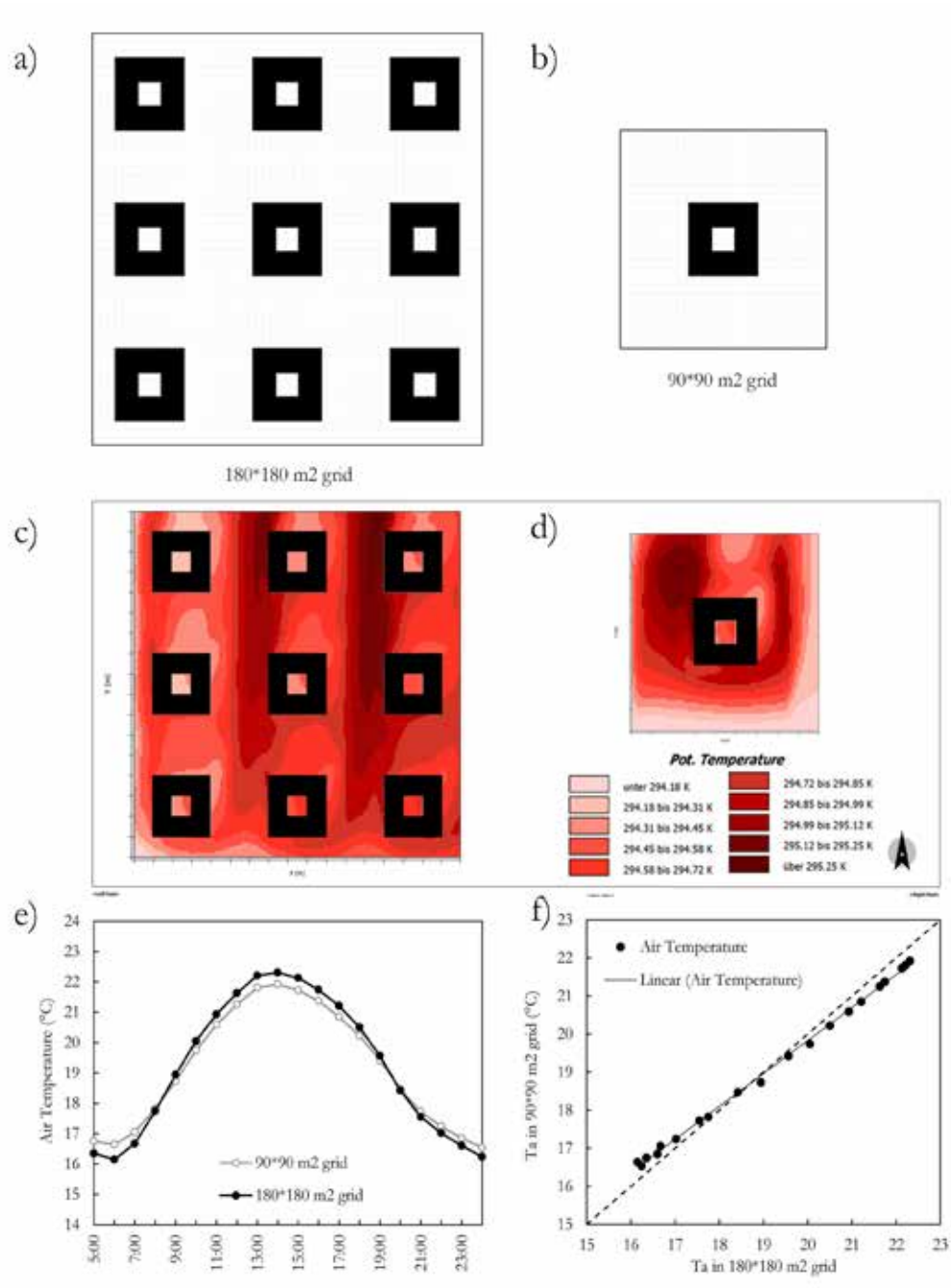

Figure 8

*a) the courtyard model 10*10 m² in 180*180 domain size with similar neighbouring blocks, b) the same courtyard model withought neighbours and in 90*90 domain size, c) the air temperature in 180*180 domain size on 19th of June 2000, d) the air temperature in 90*90 domain size in the same day e) the air temperatures compared in different domain sizes, f) scatterplot of air temperature in 90*90 versus 180*180.*

ENVI-met as a CFD program has been previously validated in different climates and countries such as Germany (Freiburg) [74], China (Guangzhou) [76], Singapore (Singapore) [77], Japan (Saga) [78], Morroco (Fez) [54] USA (Phoenix) [79], and UAE (Dubai) [80]. The programmer of ENVI-met states that because the vertical long-wave flux divergence is not taken into account, this could result in a temperature difference of 2 to 4 °C between measurement and simulation [81]. In this research, ENVI-met is also validated for a case in the Netherlands. The maximum deviation of the simulation from the measurements is 2.5°C at 10:00 AM. Moreover, because ENVI-met does not consider cloudiness of sky, simulation of sunny days could be more realistic. In the boundry sensitivity check process, making the reference models when they are standing alone versus in a larger context with neighbouring blocks, showed small differences in air temperature. Therefore, the rest of the simulations in this research are with the mentioned knowledge on reliability about ENVI-met as the research tool.

§ 7.3 Results and discussion

As explained, the five models were simulated for the hottest day in the reference year. The duration of insolation on the reference points are depicted in Figure 9. Insolation stands for incident solar radiation. As shown in Table 5 summarising the duration of insolation, the reference points at the centre of the a), b) and c) models receive solar radiation for the longest period, whilst the linear N-S oriented and the courtyard receive solar radiation during a much shorter period. Moreover, the sky views from the reference points are also illustrated in Figure 9.

Considering the microclimates in these reference points, Figure 10 shows the air temperature and wind speed at the hottest time of the reference year for these models. Comparing air temperature and wind velocity in these models, the singular models (a and b) are simultaneously more exposed to the sun and the wind from the South (187°). Referring to Figure 11, the centre of the models a) and b) have the highest mean radiant temperature among the models. Likewise, the linear E-W model has a long duration of direct sun. The difference between this model and the singular ones concerning solar radiation occurs between 11:00 h and 14:00 h. During this period, the mean radiant temperature of the linear E-W model decreases since the direct rays of the sun are blocked by the roof edge of the lower linear block reducing solar radiation onto the reference point. Furthermore, when the sun rays appear again from behind the obstacle, the mean radiant temperature rises to the same temperature as at 11:00 h.

In contrast, the linear N-S model (d) shows different behaviour. Before 11:00 h, the central point is protected by the surrounding buildings and T_{mrt} increases with a low slope. Between 10:00 h and 14:00 h, it receives direct sun and T_{mrt} increases very fast.

Similarly, the courtyard model (e) has the same increase in T_{mrt}; however, its peak is lower than that of the linear N-S model. This is due to the blockage of the sun by the south façade of the courtyard.

Model	Insolation start - end	Total duration
Singular blocks E-W	06:00 - 18:38	12h:38m
Singular blocks N-S	06:00 - 18:38	12h:38m
Linear blocks E-W	06:24 - 18:14	11h:50m
Linear blocks N-S	10:03 - 14:35	04h:32m
Courtyard block	10:03 - 14:35	04h:32m

Table 5
The duration of insolation of the reference points in the models on the 19th of June.

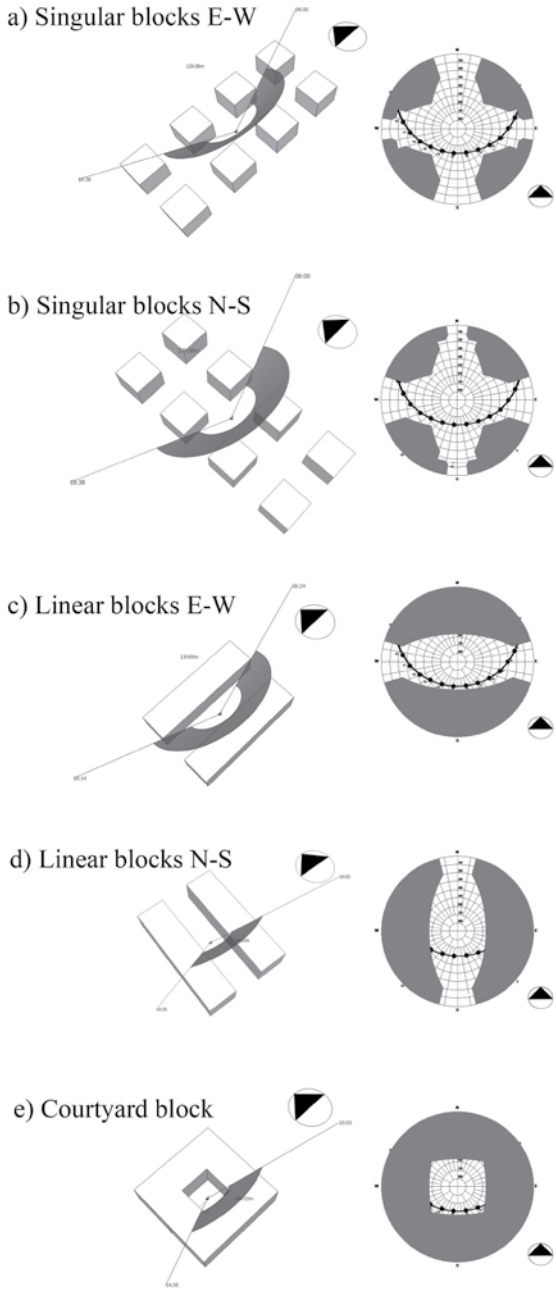

Figure 9
Left: insolation of the models; Right: sky views from the reference points (the images are generated by the Chronolux plug-in for Sketchup and by RayMan, respectively).

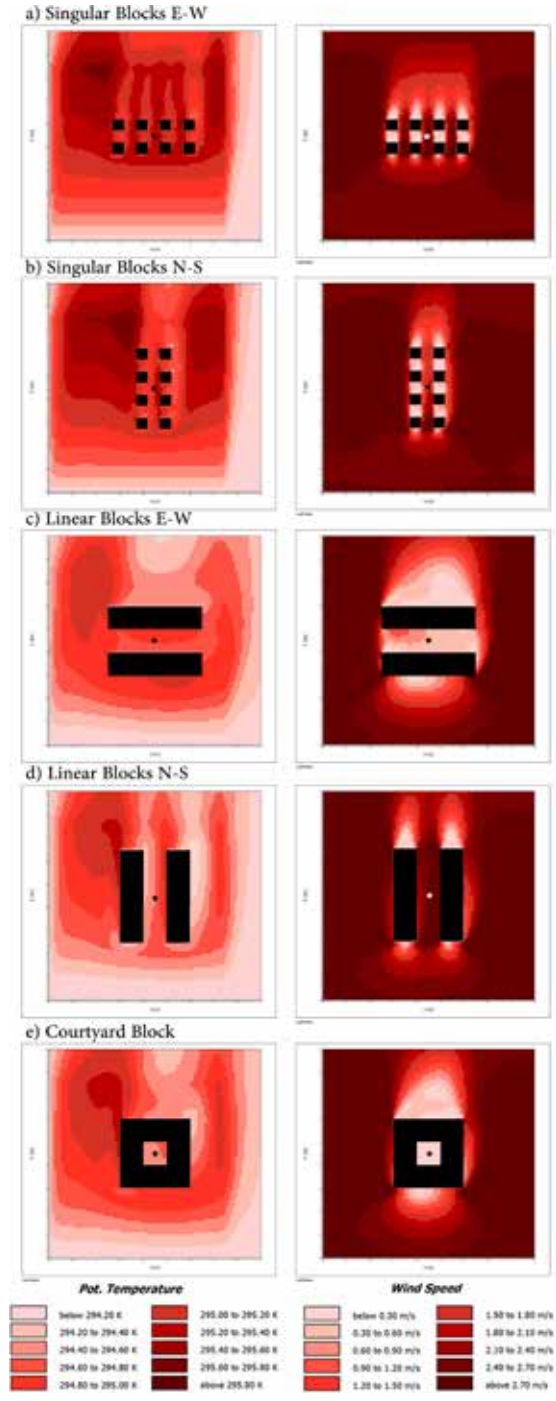

Figure 10
Air temperatures (left) and local air velocities (right) at 16:00h on the 19th of June.

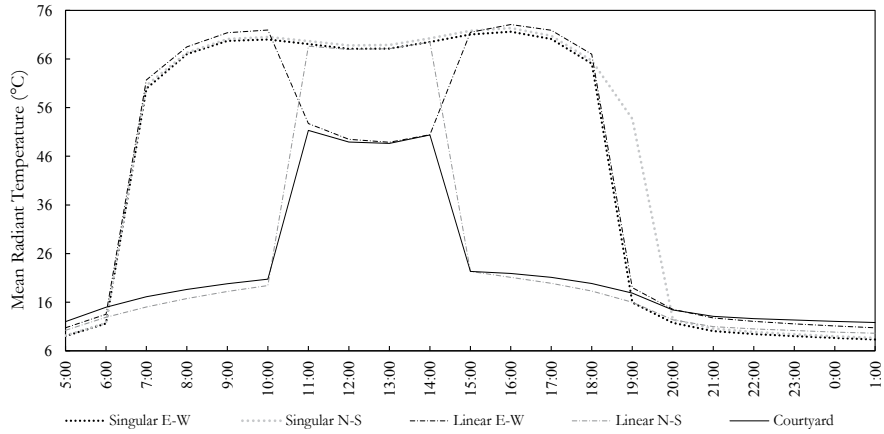

Figure 11
Mean radiant temperatures (T_{mrt}) at the reference points.

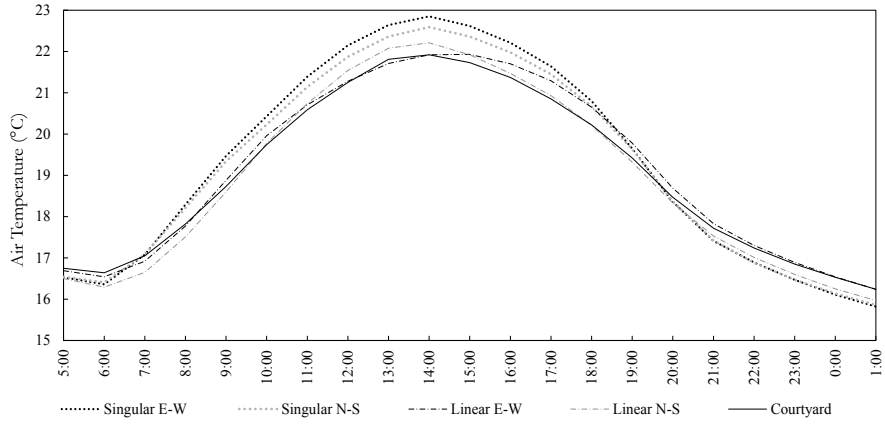

Figure 12
Air temperatures (T_a) at the reference points.

Comparing the compactness of the models with their microclimate behaviour during the day, their average T_{mrt} is described in Table 6. T_{mrt} and T_a for the simulated day are also depicted in Figures 11 and 12, respectively. Moreover, the standard deviation of the T_{mrt} is also calculated for each model. In this regard, from the singular E-W model to the courtyard model, the compactness is decreasing. In parallel, the average T_{mrt} and its standard deviation is also decreasing. This indicates that the average T_{mrt} is relevant to the openness to the sky in the form of a positive correlation. In other words, the greater the compactness, the higher the protection from the sun.

Regarding wind within the microclimates, the average wind speeds are described in Table 6. Figure 13 also shows the hourly differences among the models. The prevailing wind direction on this day is South-West (187°). Looking at the results and comparing the singular, the linear and the courtyard models, the average wind speed reduces from singular to courtyard model, respectively. In other words, the more open the form, the more exposed it is to wind. Moreover, the orientation of the models plays an important role as well. As an illustration, although the singular N-S form is an open form, the receptor point in the canyon is protected from the South-West wind by the spread cubes. However, as Figure 10 shows, the central point in the canyon is less protected from the prevailing wind. This situation is reversed for the linear forms. The E-W form blocks the wind, while the N-S form allows the wind to cross the canyon easier. On this account, the courtyard has the lowest wind speed (0.2 m/s) and as a result the most protected microclimate.

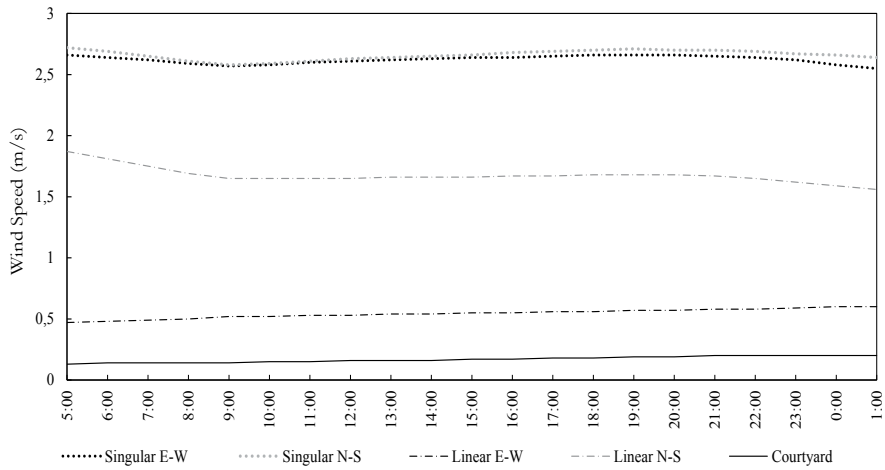

Figure 13
Wind speed at the reference points.

This chapter evaluates thermal comfort for pedestrians in the outdoor environment with five different urban forms. As mentioned in the literature review, physiological equivalent temperature (PET) is the most accurate and common index used in Western and Northern Europe [11, 42, 82]. Therefore, the PET at the central point of the models (for the hottest day in De Bilt) was calculated and illustrated in Figure 14. The results of PET are roughly similar to T_{mrt}, because the mean radiant temperature has a direct relationship with thermal comfort [36, 83].

	Singular E-W	Singular N-S	Linear E-W	Linear N-S	Courtyard
SVF	0.605	0.605	0.404	0.404	0.194
Average T_a (°C)	19.3	19.2	19.1	18.9	19.0
Average T_{mrt} (°C)	43.5	45.8	41.6	25.1	22.9
Standard deviation of T_{mrt} (°C)	28.8	28.3	26.0	21.4	13.5
Average wind (m/s)	2.6	1.7	0.5	2.7	0.2
PET	23.5	26.4	27.2	17	20.8
Comfortable hours *	3	2	4	8	17

Table 6

*Averages of the microclimates properties. *= The sum of slightly cool, comfortable and slightly warm hours.*

The results show that during the reference day, the central points inside the linear N-S and courtyard models have the lowest average PET among the models. The courtyard has also the smallest standard deviation of T_{mrt}. In Figure 14, the comfort bandwidths are highlighted with a grey rectangle covering 13°C to 29°C of PET (from slightly cool to slightly warm). As shown here, the courtyard block provides 17 thermally comfortable hours. The second most comfortable model is the linear N-S with only 4.5 hours of direct sun. The elongation of this model is in accordance with the prevailing wind and this provides an average wind speed of 2.7 m/s in the reference point which helps to reduce heat stress. The singular models provide 2 or 3 hours of thermal comfort. Looking at Figure 11, their mean radiant temperatures increase at 06:00 h, remain at the hottest temperature because of the direct sun, and drop down around 19:00 h.

Considering Figures 15 (PET in microclimates) and 5 (PET in the city) allows comparing PET inside microclimates and city climate (open field). Based on these two graphs very cold and cold situations do not occur inside the microclimates, and very hot and hot situations do not occur in the city climate. Apparently in the open field (city climate), the parameters affecting thermal comfort (such as wind) are leading to a cooler environment. To be more precise, a very hot situation only occurs in the linear E-W model.

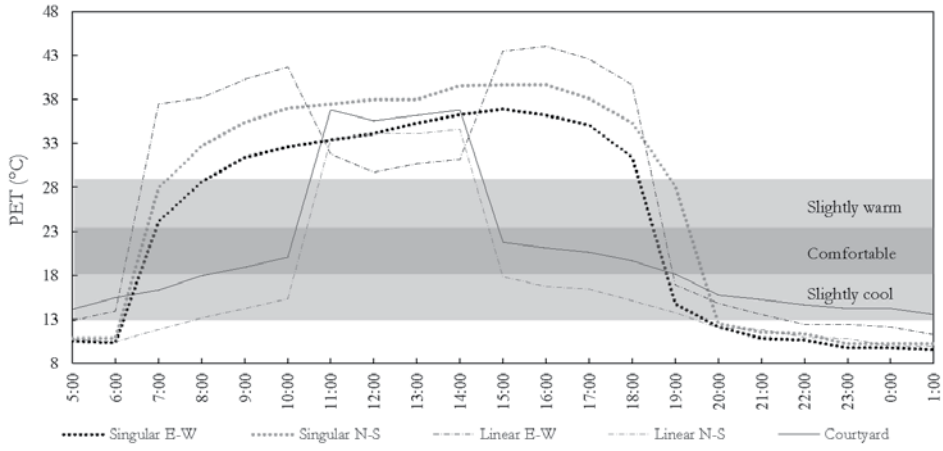

Figure 14
PET at the reference points (the comfort range is highlighted with grey).

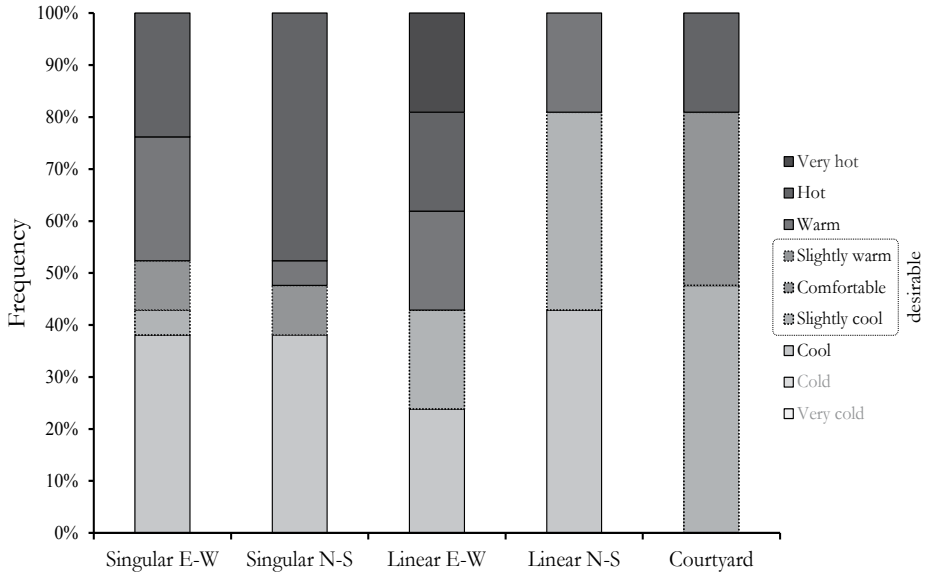

Figure 15
Percentage frequency of PET in accordance with Figure 12 at the reference points.

§ 7.4 Conclusions

A comparison between the models and their outdoor thermal comfort situations can generate clear guidelines for landscape and urban designers who want to create thermally comfortable outdoor climates. The three main urban forms studied (singular, linear and courtyard), each with a different compactness, provide different situations in their microclimate. Among different parameters that affect outdoor thermal comfort, mean radiant temperature and wind velocity are influenced more by urban geometry.

The results of this chapter showed that in the temperate climate of the Netherlands, the singular shapes provide a long duration of solar radiation for the outdoor environment. This causes the worst comfort situation among the models at the centre of the canyon. In contrast, the courtyard provides a more protected microclimate which has less solar radiation in summer. Considering the physiological equivalent temperature (PET), the courtyard has the most comfortable hours on a summer day. Since courtyards are not yet very common in temperate climates, the changing global climate, with an expected increase of temperature levels in Western Europe, advocates the usage of courtyards in (new or redeveloped) urban settings.

Regarding the different orientations of the models and their effect on outdoor thermal comfort, it is difficult to specify the differences between the singular E-W and N-S forms because they receive equal amounts of insolation and are equally exposed to wind. Nevertheless, the linear E-W and N-S forms are different in their thermal behaviour. The centre point at the linear E-W form receives sun for about 12 hours a day. In contrast, this point at the linear N-S form receives 4 hours of direct sunlight per day. Therefore, in comparison with the E-W orientation this N-S orientation provides a cooler microclimate.

Finally, our recommendation for further research on the courtyard as an optimal urban form is to study the effects of different orientations on insolation and different aspect ratios (length to width and height to width) on the microclimate. Another parameter that plays an important role in the urban microclimate is vegetation. Trees and deciduous trees in particular can protect spaces from direct sun in summer and allow solar radiation in winter. Vegetation also has a low heat capacity. Referring back to the PET which illustrates thermal comfort, it increases in the afternoon. This is because the heat stored during the day is released to the air during the afternoon and evening. More investigations are needed to show whether green areas with a lower heat capacity (over construction materials) can minimise the canyon temperature.

Appendix

Mean radiant temperature (T_{mrt}) is calculated by ENVI-met. This factor sums up all short and long wave radiation fluxes (direct and reflected) on a specific point. This parameter is calculated with the following equation:

$$T_{mrt} = \left[(GT + 273.15)^4 + \frac{1.1*10^8*v_a^{0.6}}{\delta*D^{0.4}}(GT - T_a)\right]^{0.25} - 273.15 \quad (4)$$

Where

T_{mrt} is the mean radiant temperature (K),
GT is the globe temperature (K),
v_a is the air velocity near the globe (m/s)
δ is the emissivity of the globe which normally is assumed 0.95,
D is the diameter of the globe (m) which typically is 0.15 m, and
T_{a} is the air temperature (K).

ENVI-met, the software tool used for this chapter, divides the surrounding enclosure into "n" isothermal surfaces. The equation used by ENVI-met for calculating T_{mrt} is Ali-Toudert and Mayer [53]:

$$T_{mrt} = \left[\frac{1}{\sigma}\left(\sum_{i=1}^{n} E_i F_i + \frac{\alpha_k}{\varepsilon_p}\sum_{i=1}^{n} D_i F_i + \frac{\alpha_k}{\varepsilon_p} f_p I\right)\right]^{0.25} \quad (5)$$

Where

E_i is the long wave radiation (W),
D_i is the diffuse and diffusely reflected short wave radiation (W),
F_i is the angle weighting factor,
I is the direct solar radiation (W),
f_p is the surface projection factor,
α_k is the absorption coefficient of the irradiated body surface for short wave radiation,
ε_p is the emissivity of the human body, and
σ is the Stefan–Boltzmann constant ($5.67 * 10^{-8}$ W/m^{2}K^4).

Finally, T_{mrt} in ENVI-met is calculated for each grid point (z) via:

$$T_{mrt} = \left[\frac{1}{\sigma}\left(E_t(z) + \frac{\alpha_k}{\varepsilon_p}(D_t(z) + I_t(z))\right)\right]^{0.25} \quad (6)$$

References

1 ISO. International Standard 7730. ISO Geneva, revised 1990; 1984.

2 Oke TR. Boundary Layer Climates. New York: Routledge; 1987.

3 Givoni B. Climate Considerations in Building and Urban Design: Wiley; 1998.

4 Tseliou A, Tsiros IX, Lykoudis S, Nikolopoulou M. An evaluation of three biometeorological indices for human thermal comfort in urban outdoor areas under real climatic conditions. Building and Environment. 2010;45:1346-52.

5 Herrmann J, Matzarakis A. Mean radiant temperature in idealised urban canyons—examples from Freiburg, Germany. Int J Biometeorol. 2012;56:199-203.

6 Chen L, Ng E. Outdoor thermal comfort and outdoor activities: A review of research in the past decade. Cities. 2012;29:118-25.

7 Cohen P, Potchter O, Matzarakis A. Human thermal perception of Coastal Mediterranean outdoor urban environments. Applied Geography. 2013;37:1-10.

8 Andreou E. Thermal comfort in outdoor spaces and urban canyon microclimate. Renewable Energy. 2013;55:182-8.

9 Taleghani M, Tenpierik M, Kurvers S, van den Dobbelsteen A. A review into thermal comfort in buildings. Renewable and Sustainable Energy Reviews. 2013;26:201-15.

10 Höppe P. Different aspects of assessing indoor and outdoor thermal comfort. Energy and Buildings. 2002;34:661-5.

11 Matzarakis A, Mayer H, Iziomon MG. Applications of a universal thermal index: physiological equivalent temperature. Int J Biometeorol. 1999;43:76-84.

12 Blazejczyk K, Broede P, Fiala D, Havenith G, Holmer I, Jendritzky G, et al. Priciples of the new universal thermal cliamte index (UTCI) and its application to bioclimatic research in European scale. Miscellanea Geographica. 2010;14:91-102.

13 Change IPoC. Climate Change 2007 - The Physical Science Basis: Contribution of Working Group I to the Fourth Assessment Report of the IPCC. Cambridge2007.

14 Johansson E, Thorsson S, Emmanuel R, Krüger E. Instruments and methods in outdoor thermal comfort studies – The need for standardization. Urban Climate.

15 Howard L. The climate of London, deduced from meteorological observations made in the metropolis and various places around it. London: Harvey and Darton; 1833.

16 Hill L, Griffith OW, Flack M. The Measurement of the Rate of Heat-Loss at Body Temperature by Convection, Radiation, and Evaporation. Philosophical Transactions Research Society London B. 1916;207:183-220.

17 Dufton AF. The eupatheostat. Scientific Instruments. 1929;6:249-51.

18 Yongping J, Jiuxian M. Evolution and evaluation of research on the relation between room airflow and human thermal comfort. Journal of Heating Ventilating & Air Conditioning. 1999;29:27-30.

19 Ouzi L, Yuli H, Xunqian L. Study of thermal comfort of occupants and indoor air quality—historical review, present status and prospects. Building Energy & Environment. 2001;21:26-8.

20 Hanqing W, Chunhua H, Zhiqiang L, Guangfa T, Yingyun L, Zhiyong W. Dynamic evaluation of thermal comfort environment of air-conditioned buildings. Building and Environment. 2006;41:1522-9.

21 Fanger P. Thermal Comfort: Analysis and Applications in Environmental Engineering. Copenhagen Danish Technical Press; 1970.

22 Tahbaz M. Psychrometric chart as a basis for outdoor thermal analysis. International Journal of Architectural Engineering & Urban Planning. 2011;21:95-109.

23 Belding HS, Hatch TF. Index for evaluating heat stress in terms of resulting physiological strain. Heating, piping, and air conditioning. 1955;27:129-36.
24 Yaglou CP, Minard D. Control of heat casualties at military training centers. AMA ArchIndustrHealth. 1957;16:302-16.
25 Thom EC. The Discomfort Index. Weatherwise. 1959;12:57-61.
26 Givoni B. The influence of work and environmental conditions on the physiological responses and thermal equilibrium of man. f UNESCO Symposium on Environmental Physiology and Psychology in Arid Conditions. Lucknow1962. p. 199-204.
27 Gagge AP, Stolwijk JAJ, Nishi Y. Effective temperature scale, based on a simple model of human physiological regulatory response. ASHRAE. 1971;13.
28 Kerslake DM. The stress of hot environment. Cambridge: Cambridge University Press; 1972.
29 Steadman RG. The Assessment of Sultriness. Part I: A Temperature-Humidity Index Based on Human Physiology and Clothing Science. Journal of Applied Meteorology and Climatology. 1979;18:861-73.
30 Sharma MR, Ali S. Tropical summer index—a study of thermal comfort of Indian subjects. Building and Environment. 1986;21:11-24.
31 ISO/TR11079. Evaluation of cold environments – Determination of required clothing insulation (IREQ). Geneva: International Organization for Standardisation; 1993.
32 Gagge AP, Fobelets AP, Berglund LG. A standard predictive index of human response to the thermal environment. ASHRAE Transaction 921986. p. 709-31.
33 Staiger H, Bucher K, Jendritzky G. Gefühlte Temperatur. Die physiologisch gerechte Bewertung von Wärmebelastung und Kältestress beim Aufenthalt im Freien in der Maßzahl Grad Celsius. Annalen der Meteorologie. 1997;33:100-7.
34 Pickup J, de Dear RJ. An outdoor thermal comfort index (OUT_SET*) – part I – the model and its assumptions. In: R. J. de Dear, J. D. Kalma, T. R. Oke, Auliciems A., editors. Selected papers from the ICB-ICUC'99 conference, Sydney. Geneva: World Meteorological Organization; 2000.
35 Mayer H, Höppe P. Die Bedeutung des Waldes für die Erholung aus der Sicht der Humanbioklimatologie. Forstwissenschaftliches Centralblatt. 1984;103:125-31.
36 Höppe P. The physiological equivalent temperature - A universal index for the biometeorological assessment of the thermal environment. Int J Biometeorol. 1999;43:71-5.
37 Jendritzky G, Maarouf A, Henning S. Looking for a Universal Thermal Climate Index UTCI for Outdoor Applications. Windsor Conference on Thermal Standards. Windsor, UK: Network for Comfort and Energy Use in Buildings; 2001.
38 Fiala D, Havenith G, Bröde P, Kampmann B, Jendritzky G. UTCI-Fiala multi-node model of human heat transfer and temperature regulation. Int J Biometeorol. 2012;56:429-41.
39 Bröde P, Fiala D, Bła ejczyk K, Holmér I, Jendritzky G, Kampmann B, et al. Deriving the operational procedure for the Universal Thermal Climate Index (UTCI). Int J Biometeorol. 2012;56:481-94.
40 Höppe P. Heat balance modelling. Experientia. 1993;49:741-6.
41 Blazejczyk K, Epstein Y, Jendritzky G, Staiger H, Tinz B. Comparison of UTCI to selected thermal indices. Int J Biometeorol. 2012;56:515-35.
42 Matzarakis A, Amelung B. Physiological Equivalent Temperature as Indicator for Impacts of Climate Change on Thermal Comfort of Humans. In: Thomson M.C., García Herrera R., Beniston M., editors. Seasonal Forecasts, Climatic Change and Human Health: Springer; 2008.
43 Olgyay V. Design with Climate. Princeton NJ: Princeton University Press; 1963.
44 Steemers K, Baker N, Crowther D, Dubiel J, Nikolopoulou MH, Ratti C. City texture and microclimate. Urban Design Studies. 1997;3:25-50.

45 Ratti C, Raydan D, Steemers K. Building form and environmental performance: archetypes, analysis and an arid climate. Energy and Buildings. 2003;35:49-59.
46 Bourbia F, Awbi HB. Building cluster and shading in urban canyon for hot dry climate: Part 1: Air and surface temperature measurements. Renewable Energy. 2004;29:249-62.
47 Bourbia F, Awbi HB. Building cluster and shading in urban canyon for hot dry climate: Part 2: Shading simulations. Renewable Energy. 2004;29:291-301.
48 Yezioro A, Capeluto IG, Shaviv E. Design guidelines for appropriate insolation of urban squares. Renewable Energy. 2006;31:1011-23.
49 Berkovic S, Yezioro A, Bitan A. Study of thermal comfort in courtyards in a hot arid climate. Solar Energy. 2012;86:1173-86.
50 Okeil A. In search for Energy efficient urban forms: the residential solar block. the 5th International Conference on Indoor Air Quality, Ventilation and Energy Conservation in Buildings Proceedings. Toronto2004.
51 Okeil A. A holistic approach to energy efficient building forms. Energy and Buildings. 2010;42:1437-44.
52 Ali-Toudert F, Mayer H. Effects of asymmetry, galleries, overhanging façades and vegetation on thermal comfort in urban street canyons. Solar Energy. 2007;81:742-54.
53 Ali-Toudert F, Mayer H. Numerical study on the effects of aspect ratio and orientation of an urban street canyon on outdoor thermal comfort in hot and dry climate. Building and Environment. 2006;41:94-108.
54 Johansson E. Influence of urban geometry on outdoor thermal comfort in a hot dry climate: A study in Fez, Morocco. Building and Environment. 2006;41:1326-38.
55 Bourbia F, Boucheriba F. Impact of street design on urban microclimate for semi arid climate (Constantine). Renewable Energy. 2010;35:343-7.
56 Erell E, Pearlmutter D, Williamson TJ. Urban Microclimate: Designing the Spaces Between Buildings: Earthscan; 2012.
57 Shashua-Bar L, Pearlmutter D, Erell E. The cooling efficiency of urban landscape strategies in a hot dry climate. Landscape and Urban Planning. 2009;92:179-86.
58 Taleghani M, Sailor DJ, Tenpierik M, van den Dobbelsteen A. Thermal assessment of heat mitigation strategies: The case of Portland State University, Oregon, USA. Building and Environment. 2014;73:138-50.
59 Taleghani M, Tenpierik M, Dobbelsteen A. Environmental Impact of Courtyards- A Review and Comparison of Residential Courtyard Buildings in Different Climates. Green Building. 2012;7:113-36.
60 Müller N, Kuttler W, Barlag A-B. Counteracting urban climate change: adaptation measures and their effect on thermal comfort. Theor Appl Climatol. 2013:1-15.
61 Thorsson S, Lindberg F, Björklund J, Holmer B, Rayner D. Potential changes in outdoor thermal comfort conditions in Gothenburg, Sweden due to climate change: the influence of urban geometry. International Journal of Climatology. 2011;31:324-35.
62 Taleghani M, Tenpierik M, van den Dobbelsteen A, de Dear R. Energy use impact of and thermal comfort in different urban block types in the Netherlands. Energy and Buildings. 2013;67:166-75.
63 Taleghani M, Tenpierik M, van den Dobbelsteen A. Energy performance and thermal comfort of courtyard/atrium dwellings in the Netherlands in the light of climate change. Renewable Energy. 2014;63:486-97.
64 Taleghani M, Tenpierik M, van den Dobbelsteen A, Sailor DJ. Heat in courtyards: A validated and calibrated parametric study of heat mitigation strategies for urban courtyards in the Netherlands. Solar Energy. 2014;103:108-24.

65 van Esch MME, Looman RHJ, de Bruin-Hordijk GJ. The effects of urban and building design parameters on solar access to the urban canyon and the potential for direct passive solar heating strategies. Energy and Buildings. 2012;47:189-200.
66 NEN-5060. Hygrothermische Eigenschappen van Gebouwen Referentieklimaatgegevens. Nederlands Normalisatie-Instituut (NNI); 2008.
67 Matzarakis A, Rutz F, Mayer H. Modelling radiation fluxes in simple and complex environments—application of the RayMan model. Int J Biometeorol. 2007;51:323-34.
68 Martin L, March L. Urban Space and Structures. UK: Cambridge University Press; 1972.
69 Bruse M. Die Auswirkungen kleinskaliger Umweltgestaltung auf das Mikroklima, Entwicklung des prognostischen numerischen Modells ENVI-met zur Simulation der Wind-, Temperatur-, und Feuchtverteilung in sta¨dtischen Strukturen: University of Bochum, Germany; 1999.
70 Lindberg F, Holmer B, Thorsson S. SOLWEIG 1.0 – Modelling spatial variations of 3D radiant fluxes and mean radiant temperature in complex urban settings. Int J Biometeorol. 2008;52:697-713.
71 Defraeye T, Blocken B, Carmeliet J. CFD simulation of heat transfer at surfaces of bluff bodies in turbulent boundary layers: Evaluation of a forced-convective temperature wall function for mixed convection. Journal of Wind Engineering and Industrial Aerodynamics. 2012;104–106:439-46.
72 Wania A, Bruse M, Blond N, Weber C. Analysing the influence of different street vegetation on traffic-induced particle dispersion using microscale simulations. Journal of Environmental Management. 2012;94:91-101.
73 Bruse M. Simulating microscale climate interactions in complex terrain with a high-resolution numerical model: A case study for the Sydney CBD Area. Biometeorology and Urban Climatology at the Turn of the Millennium, WMO/TD No 1026. World Meteorological Organisation, Geneva, CH2000.
74 Bruse M, Fleer H. Simulating surface–plant–air interactions inside urban environments with a three dimensional numerical model. Environmental Modelling & Software. 1998;13:373-84.
75 Kottek M, Grieser J, Beck C, Rudolf B, Rubel F. World Map of the Köppen-Geiger climate classification updated. Meteorologische Zeitschrift. 2006;15.
76 Yang X, Zhao L, Bruse M, Meng Q. Evaluation of a microclimate model for predicting the thermal behavior of different ground surfaces. Building and Environment. 2013;60:93-104.
77 Wong NH, Kardinal Jusuf S, Aung La Win A, Kyaw Thu H, Syatia Negara T, Xuchao W. Environmental study of the impact of greenery in an institutional campus in the tropics. Building and Environment. 2007;42:2949-70.
78 Srivanit M, Hokao K. Evaluating the cooling effects of greening for improving the outdoor thermal environment at an institutional campus in the summer. Building and Environment. 2013;66:158-72.
79 Hedquist BC, Brazel AJ. Seasonal variability of temperatures and outdoor human comfort in Phoenix, Arizona, U.S.A. Building and Environment.
80 Taleb D, Abu-Hijleh B. Urban heat islands: Potential effect of organic and structured urban configurations on temperature variations in Dubai, UAE. Renewable Energy. 2013;50:747-62.
81 Bruse M, BÜRGER M, Bohnstedt A, Ihde A, Jesionek K, Lahme E. Measurements and model simulations in WP MICRO. Ruhr-University Bochum, Institute of Geography, Research Group Climatology2002.
82 Hwang RL, Lin TP, Matzarakis A. Seasonal effects of urban street shading on long-term outdoor thermal comfort. Building and Environment. 2011;46:863-70.
83 Thorsson S, Lindberg F, Eliasson I, Holmer B. Different methods for estimating the mean radiant temperature in an outdoor urban setting. International Journal of Climatology. 2007;27:1983-93.

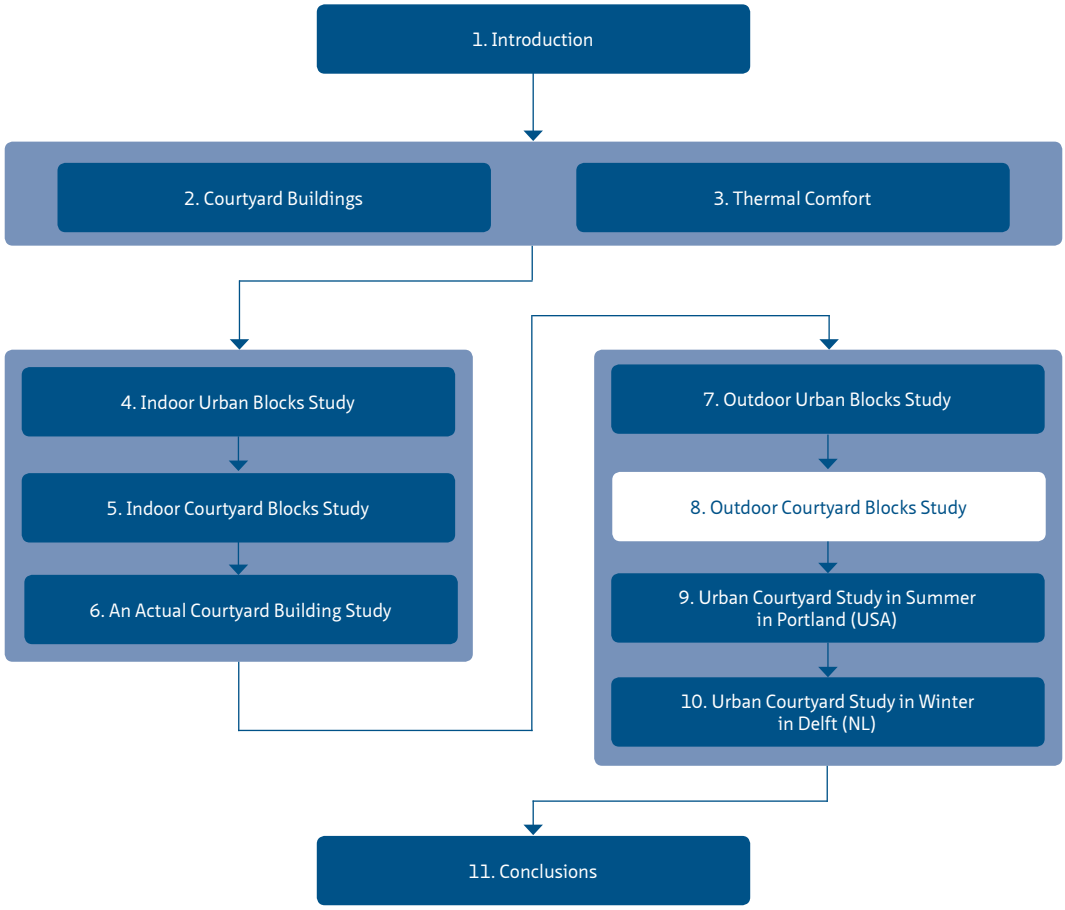
1. Introduction
2. Courtyard Buildings
3. Thermal Comfort
4. Indoor Urban Blocks Study
5. Indoor Courtyard Blocks Study
6. An Actual Courtyard Building Study
7. Outdoor Urban Blocks Study
8. Outdoor Courtyard Blocks Study
9. Urban Courtyard Study in Summer in Portland (USA)
10. Urban Courtyard Study in Winter in Delft (NL)
11. Conclusions